

77-8-317
高工研圖書室

DEUTSCHES ELEKTRONEN-SYNCHROTRON **DESY**

DESY 77/53
August 1977

Experimental Results in Photoproduction

by

Christoph Berger

I. Physikalisches Institut, Technische Hochschule Aachen

NOTKESTRASSE 85 · 2 HAMBURG 52

To be sure that your preprints are promptly included in the
HIGH ENERGY PHYSICS INDEX ,
send them to the following address (if possible by air mail) :

DESY
Bibliothek
2 Hamburg 52
Notkestieg 1
Germany

EXPERIMENTAL RESULTS IN PHOTOPRODUCTION

Christoph Berger
I. Physikalisches Institut
Technische Hochschule Aachen
Germany

Invited talk at the
European Conference on Particle Physics
Budapest, Hungary
4-9 July 1977

EXPERIMENTAL RESULTS IN PHOTOPRODUCTION

Ch. Berger, I. Physikalisches Institut der RWTH Aachen, Germany

Introduction

Looking at the topics of this conference one can roughly divide the experiments in lepton induced and hadron induced reactions. In this context photoproduction plays an important role because on one hand one knows from many experiments about the hadronic nature of the photon, on the other hand photoproduction is the $Q^2 = 0$ limit of electroproduction.

In the last two years we did not have very spectacular news in the field of classical photoproduction below 20 GeV, but new experiments have refined our picture of photon induced reactions and many experiments only known from preprints and conference contributions have been published in their final form.

1. Total cross section and related topics

To my knowledge there are no new measurements of the total cross section below $E_\gamma = 20$ GeV (1), but we have new information on the difference $\sigma_{tot}(\gamma p) - \sigma_{tot}(\gamma n)$ from compton scattering and ω meson production.

The amplitude for proton and neutron compton scattering can be written

$$\begin{aligned} T_{\gamma p} &= T_0 + T_1 \\ T_{\gamma n} &= T_0 - T_1 \end{aligned}$$

where T_0 and T_1 describe $l = 0$ and $l = 1$ t-channel exchange respectively. Via the optical theorem we get

$$\frac{\sigma_{tot}(\gamma p) - \sigma_{tot}(\gamma n)}{\sigma_{tot}(\gamma p) + \sigma_{tot}(\gamma n)} = \epsilon = \frac{\text{Im } T_1(t=0)}{\text{Im } T_0(t=0)}$$

The $l = 1$ amplitude is usually assumed to be dominated by A_2 exchange and the small measured value of ϵ (e.g. $\epsilon = 5\%$ at $E_\gamma = 4$ GeV) gives a small A_2 contribution. But following an argument of Harari (2) even a small ϵ leads to a large effect in ω production in forward direction: The natural parity exchange part of the cross sections given by

$$\frac{d\sigma}{dt} \Big|_{t=0}(\gamma p \rightarrow \omega p) = |A_0|^2 (1 + \delta)$$

with $\delta = \text{Im } A_1 / \text{Im } A_0$ (putting $\text{Re } A_0 = 0$ and $|A_0|^2 \gg |A_1|^2$) The phase δ is related to ϵ via vector meson dominance (VMD). In the simplest case (3) we have

$$\delta = \frac{f_\omega^2}{f_\rho^2} \cdot \epsilon$$

where f_ω^2, f_ρ^2 are the usual photon-vector-meson coupling constants (fig.1). Because $f_\omega^2/f_\rho^2 \approx 8$ one expects a rather large effect even for small values of ϵ . The most recent data came from experiments at Daresbury (4) ($E_\gamma = 3.9$ GeV) and Cornell (5) ($E_\gamma = 8.5$ GeV). Fig.2 is taken from ref. 4 and shows all measurements of δ combined. The shaded area is the expectation from total cross section experiments. Only at the highest energy the simple mechanism explained above seems to work, whereas at low energies the A_2 exchange amplitude evaluated from ω production is too small to account for the difference of $\sigma_{tot}(\gamma p)$ and $\sigma_{tot}(\gamma n)$.

By measuring compton scattering on hydrogen and deuterium in forward direction one can determine $|T_1|^2/|T_0|^2 + |T_1|^2$ and

$R_e(T_0 T_1^*) / |T_0 + T_1|^2$. A group at DESY has carried out an experiment (6) at $E_\gamma = 5$ and $E_\gamma = 6$ GeV. Their result together with the result of other experiments is given in table 1. All ratios are compatible with a small $l = 1$ exchange contribution to the photon nucleon interaction.

11. Shadowing

The total photon nucleon absorption cross section has the rather small value of 120 μb . Therefore the mean free path in nuclear matter is large and one expects the absorption cross section in nuclei to be proportional to the atomic weight number A

$$\sigma_{\text{tot}}(\gamma A) = A \sigma_{\text{tot}}(\gamma N).$$

It is a well known fact that in contrast to this expectation many experiments (7) have seen shadowing i.e.

$$\frac{\sigma_{\text{tot}}(\gamma A)}{\sigma_{\text{tot}}(\gamma N)} = A_{\text{eff}} < A$$

This effect is due to the hadronic nature of the photon. Using VMD one can calculate A_{eff} quantitatively. Especially VMD predicts a transition energy E_γ below which shadowing is small and above which shadowing is complete. ($A_{\text{eff}} = A^{2/3}$) like in hadronic interactions. This transition energy is roughly given by

$$E_\gamma = m_\nu^2 \cdot \lambda_\nu \quad (1)$$

where m_ν is the vector meson mass and λ_ν its mean free path in nuclear matter (8) ($E_\gamma \approx 6$ GeV for ρ mesons).

All real photon absorption experiments until now are in qualitative agreement with VMD although most of the data show less shadowing than predicted by theory and the transition effect never has been seen clearly.

The measurement of Compton scattering in complex nuclei is a more sensitive test of shadowing because $d\sigma/dt$ should be proportional to A^2 without shadowing. The results of a DESY experiment at $E_\gamma = 3$ and 5 GeV have now been published in their final form (9) (fig. 3). The full curve represents the VMD calculations taken from ref. 10. A better agreement is obtained (dashed curve) by slightly changing the input parameter σ_{pN} from 30mb to 25 mb.

A group at Cornell has just finished a new real photon shadowing experiment for energies from 2 to 10 GeV (11). They see consistently less shadowing than the average of the earlier data and they observe a clear energy dependence of A_{eff}/A at least for the heavy elements. In fig.4 their results are shown together with the data from UCSB (7). In fig. 5 I have plotted the Cornell results for Gold together with all data available from the older σ_{tot} measurements and the recent compton data from DESY (9). Although the Cornell data are higher than the other values for σ_{tot} they are certainly consistent with A_{eff} determined from the compton effect.

R.Talman, one of the authors of the Cornell experiment argues one should have much less shadowing than predicted by standard VMD (12). The main reason is what he calls 'self absorption' accounting for the fact that even a proton is a nuclear matter target of finite thickness. In fig. 4 predictions from a theory with self absorption (dashed curve) and so called standard VMD (13) (full curve) are included. I would not take the agreement of the dashed curve with the Cornell data as a very compelling evidence for 'self absorption'. Talman himself says that more generalized versions of VMD would give values of A_{eff} roughly equal to his calculations.

For virtual photons of mass Q^2 VMD predicts less shadowing at the same energy because formula (1) is replaced by

$$(Q^2 + m_V^2) \lambda_V = E_Y \quad (2)$$

At high Q^2 one has indeed almost no shadowing (14).

The Cornell group has carried out a shadowing experiment at $Q^2 = 0.1 \text{ GeV}^2$ (15). In fig. 6 A_{eff}/A is plotted versus Q^2 for $E_Y = 4 \text{ GeV}$ and $E_Y = 9 \text{ GeV}$. Compared to the older real photon experiments the Cornell data indicate a very rapid disappearance of shadowing, but together with the new results of the same group the Q^2 dependence is smooth. In conclusion I think that stretching error bars the Cornell real photon data are still compatible with the older experiments but the fact, that they are consistently higher than especially the UCSB data is very intriguing.

III. Vector meson Photoproduction

1.) Photon-Vector-Meson Coupling

By now we can include the ψ meson in to the sample of "old vector mesons" whose coupling to the photon has been seen in storage ring experiments and in photoproduction. Table 2 gives the results from storage rings including finite width corrections (16). VMD in its simplest form (represented by fig. 1) connects the forward cross section

$$\left. \frac{d\sigma}{dt} \right|_{t=0} (\gamma N + \psi N)$$

with the total vector meson nucleon cross section $\sigma_{\text{tot}} (\psi N)$

$$\left. \frac{d\sigma}{dt} \right|_{t=0} (\gamma N + \psi N) = \frac{\alpha}{16\pi} \frac{f_V^2}{4\pi} \sigma_{\text{tot}}^2 (\psi N) (1+n^2) \quad (3)$$

where n is the ratio of the real to the imaginary part of the

forward VN scattering amplitude. By using the $f_V^2/4\pi$ from the storage ring experiments and the forward cross sections from photoproduction one can calculate $\sigma_{\text{tot}} (\psi N)$ and compare it with the photoproduction measurements from complex nuclei and/or with quark model results (8). The ρ meson fits very nicely into that picture. The ω has been always more problematic (7) but one should keep in mind that for comparison with VDM one has to extract from the experiments the aforementioned $|A_0|^2$. The most recent data from Cornell (5) (8.5 GeV) and Daresbury (4) (3.9 GeV) are $|A_0|^2 = 7.4 \pm 0.5 \mu\text{b}/\text{GeV}^2$ and $14.5 \pm 5.4 \mu\text{b}/\text{GeV}^2$ respectively. Though not incompatible these values indicate the range allowed for $\sigma_{\text{tot}} (\psi N)$.

For the ϕ Meson we have the very accurate measurement of a DESY group (21). Fig. 7 shows $d\sigma/dt$ for various energies, fig. 8 $d\sigma/dt$ at $t = 0$ together with the results of older experiments. The solid line is a fit through the data just taking into account a threshold factor

$$\left. \frac{d\sigma}{dt} \right|_{t=0} = \left(\frac{p_\phi}{k_Y} \right)_{\text{CM}}^2 \left. \frac{d\sigma}{dt} \right|_{t=0, E \rightarrow \infty}$$

From this fit the authors deduce $\sigma_{\text{tot}} (\phi p) = (9.59 \pm .4) \text{ mb}$ which has to be compared to $12.5 \pm .5 \text{ mb}$ given by the quark model. The 5 standard deviation difference probably indicates that the Ansatz (3) is too simple (18).

We are lucky to have the first data on ψ production in complex nuclei from a group at SLAC (19). The muon yield coming from ψ decay (fig. 9) was detected in the SLAC 20 GeV spectrometer. From the ratio of ψ production from beryllium and tantalum targets the authors get $\sigma_{\text{tot}} (\psi N) = 3.5 \pm .8 \text{ mb}$.

The σ_{tot} value given by eq.3 is approximately 1 mb having forward cross sections measured at the same energy. This value of 1 mb is certainly pretty low compared to 3.5 mb, but at least it is in the right order of magnitude.

2. Backward Vector Meson Production

By measuring ρ^0 and f^0 production in backward direction one can isolate $l = 3/2$ and $l = 1/2$ exchanges in the u channel (fig. 10).

A group at Daresbury (20) has studied these reactions by measuring the proton in the forward direction and selecting only 3 prong events with the apparatus shown in fig. 11. The target is surrounded by wire chambers and in the forward direction there is a magnetic spectrometer including preshower-cerenkov-counters and shower counters for particle identification. The experiment was done in a 192 channel tagged photon beam with a resolution of 7 MeV/channel approximately. The group observes for both ρ^0 and f^0 production a very smooth u dependence (fig.12) with a fit giving the following results

$$\frac{d\sigma}{du} (\gamma p \rightarrow \rho^0 p) = (111 \pm 7)e^{(1.4 \pm 0.2)u} \text{ nb/GeV}^2$$

$$\frac{d\sigma}{du} (\gamma p \rightarrow f^0 p) = (174 \pm 20)e^{(1.0 \pm 0.2)u} \text{ nb/GeV}^2$$

The s dependence of the total backward production cross section ($90^\circ < \theta_{cm} < 180^\circ$) is given by

$$\sigma(\rho) \sim s^{-4.9 \pm 0.5}, \quad \sigma(f) \sim s^{-4.7 \pm 0.5}$$

The explanation of the behaviour of backward πN scattering (i.e. shrinkage, no dip in $\pi^+ p \rightarrow \pi^+ p$, dip at $u = -0.15 \text{ GeV}^2$ for

$\pi^+ p \rightarrow \pi^+ p$) has always been considered as a great success of Regge theory. In contrast to that all measurements of backward photoproduction to date ($\pi^+ n, \pi^0 p, \rho^0 p, f^0 p$) have shown no indication of the dip structure at $u = -0.15 \text{ GeV}^2$. Especially the f^0 production (pure $l = 1/2$ exchange) seems not to be dominated by reggeized nucleon exchange (N_{α^-} -trajectory).

But there is another candidate for pure $l = 1/2$ exchange: backward ω production. We have just gotten the first results on backward ω -production from the same Daresbury group which has done the ρ^0 and f^0 experiment (22). The apparatus is basically the same as used in the previous experiment. The result based on about 4500 ω events is shown in fig. 13. There is a very clear dip at $u = -0.15 \text{ GeV}^2$. In addition to that, the authors report that the backward peak is observed to shrink, and the shrinkage is consistent with that expected from the nucleon trajectory.

3. Inelastic production of ρ, ω, ϕ

A SLAC-LBL-Weizman group (25) has published data on inclusive ρ^0 production. The total cross section for $\gamma p \rightarrow \rho^0 X$ at 9.3 GeV equals $33.8 \pm 1.2 \text{ } \mu\text{b}$, where $13.3 \pm 0.5 \text{ } \mu\text{b}$ correspond to the quasi elastic channel $\gamma p \rightarrow \rho^0 p$.

The structure function $F(x_F) = \frac{1}{\pi} \frac{E^*}{p^*} \frac{d\sigma}{dx_F}$ is plotted versus x_F in fig. 14 at $E_\gamma = 9.3 \text{ GeV}$ (black points, inelastic channels only). For comparison the structure function for $\gamma p \rightarrow \pi^+ X$ is also plotted. For $x_F > 0.75$ one sees a forward diffraction dissociation peak. In order to separate diffraction dissociation from other production mechanisms the authors analyzed the decay angular distribution of the pion pairs from ρ^0 decay and found that about 60% of the cross section for $x_F > 0.8$ is due to s -channel helicity conserving ρ^0 (SCHC) events. Taking SCHC as a signature for diffraction dissociation the total

diffractive cross section at $E_Y = 9.3$ GeV is 2.7 ± 0.6 μb in agreement with a theoretical estimate by G. Wolf (38). These results give further support to the idea that SCHC is a universal property of Pomeron exchange.

Inelastic ω production has been studied by a Rochester-Cornell group (26). The function $F(x_F)$ is displayed in fig.15 for $E_Y=9.7$ GeV. At $x = 0.8$ $F(x_F)$ is about 2.5 μb compared to 5 μb for ρ^0 production. But in contrast to ρ^0 production the cross section can well be reproduced by one pion exchange (OPE) calculations whereas diffractive production is estimated to be small. On the other hand analysis of the spin density matrix does not agree with t channel helicity conservation as expected in simple OPE (26).

Inelastic cross sections $\frac{d\sigma}{dt dM^2 x}$ for ϕ production have been presented (21) by a DESY group (fig.16). The slopes are much smaller than for the quasi elastic channel $\gamma p \rightarrow \phi p$. By integration over t the authors find a ratio of inelastic to elastic production of $0.78 \pm .25$.

4. New vector mesons

A DESY-Frascati collaboration (39) has performed a new search for vector-mesons in photoproduction. The reaction $\gamma p \rightarrow e^+ e^-$ (virtual compton scattering) was studied, thus taking the $e^+ e^-$ decay of vector mesons as a unique signature. The apparatus (fig.17) consists of two identical magnetic spectrometers. The invariant mass of an $e^+ e^-$ pair is given by

$$M_{e^+e^-}^2 = 4 E_+ E_- \sin^2 \theta$$

where 2θ is the opening angle of the setup. In fig. 18 a mass spectrum for $2\theta = 130^\circ$ is given. The main background to vector meson production is the Bethe Heitler pair production. The fat solid line represents the calculated Bethe Heitler

yield above which a very clear ϕ signal is seen. (The ρ and ω are already at the acceptance limit). At the higher mass settings the $e^+ e^-$ yield cannot be attributed solely to ρ , ω , ϕ and pair production. This can be seen in fig.19 where $e^+ e^-$ yield is plotted with the QED background already subtracted.

Because of the large QED background a much more sensitive way of looking for structures in the $M_{e^+e^-}$ distribution is to study the interference term between the Bethe Heitler and the virtual compton scattering amplitude. Experimentally this is done by measuring $N_+ - N_-$, where N_+ is the number of events in a given mass bin with the e^+ having a higher transverse momentum than the e^- , (N_- resp.). The result is shown in fig.20, where the 13° , 15° and 16° degree data have been combined. Most interesting is the structure around 1100 MeV. The signal (model independent) in this mass region amounts now to 5.2 standard deviations. A narrow state of this mass is hard to explain by standard models. J. Kuti wants it to be 'gluonium'.

The next question is how to explain the large excess above $M_{e^+e^-} = 1200$ MeV. It cannot be explained by the ρ'' (1600) alone, taking the resonance parameters from photoproduction and storage ring experiments (39). The authors seem to like most a fit including 4 resonances with the fitted parameters given in table 3. One can try to identify the resonances at 1253, 1550 and 1766 MeV with the ρ' , ρ'' and ω' seen in storage ring experiments. But then again the 1443 subject is something new and it would be very interesting to see if this interpretation of the experiment can be confirmed in the future, e.g. by looking for these resonances in other channels.

IV. Pseudoscalar Meson Production

1. Exclusive reactions

We have very interesting-but preliminary-data on $\gamma p \rightarrow \pi^+ \Delta^{++}$ in backward direction from the LAMP 2 group at Daresbury (23). Because this process proceeds via pure $l = 3/2$ exchange in the u channel one can test the presence of shrinkage like seen e.g. in backward $\pi^+ p$ scattering. The experiment used a tagged photon beam in the energy range of 2.8-4.8 GeV. The apparatus (fig. 21) is a rather general set up for multiparticle detection. The preliminary results for the $\pi^+ \Delta^{++}$ channel are shown in fig.22. The 3 GeV and 4.6 GeV data show clear shrinkage. The 5.28 GeV data are earlier measurements from SLAC (24). Together with the results of backward ω production we have now two photoproduction reactions which exhibit the features of single Regge-pole dominance in the u -channel.

2. Inclusive reactions

By now we have the first data on inclusive π^+/π^- production from a polarized target in the beam fragmentation region (42) ($x_F = 0.7$ and 0.8 at $E_Y = 6$ GeV). The cross section for inclusive reactions of the type $a+b+c \rightarrow X$ has been connected to the discontinuity of the forward scattering amplitude for $a+b+c \rightarrow a+b+c$ in analogy to the usual optical theorem (40). In the beam fragmentation region this amplitude can be reggeized and one gets exchange diagrams like in fig.23.

These diagrams can be extended to the case where particle b is polarized. In a special model including cuts for the reactions $\gamma p \rightarrow \pi^+ X$ Ahmed et al (28) predicted a rather large asymmetry

$$T = \frac{d\sigma_{\uparrow} - d\sigma_{\downarrow}}{d\sigma_{\uparrow} + d\sigma_{\downarrow}}$$

The data together with the theoretical predictions are shown in fig.24. The large asymmetry is not borne out by

the experiment but at least the sign seems to be right. In an older experiment at DESY (27) the charge ratio π^+/π^- and K^+/K^- in inclusive photoproduction off the proton has been found to increase above 1 with increasing x_F and p_{\perp} . In the Mueller-Regge picture this ratio should equal 1 if only pomeron exchange contributes i.e. if the asymptotic scaling limit has been reached. Because the DESY data had been taken at $E_Y = 6$ GeV at least part of the effect can simply be due to the very low missing masses at high values of p_{\perp} . The SLAC data of Boyarski et al (28) at $E_Y = 18$ GeV have recently been published in a very thorough paper (first presentation at the Cornell Conference). Their results for the π^+/π^- ratio are shown in fig. 25. The black points are for proton target the open circles for 'neutron target' respectively. For small x_F the π^+/π^- ratio (proton target) is close to 1, but at large x_F (best seen at $x_F = .77$) it is steeply rising with p_{\perp} . In table 4 the possible exchanges for particles (+) and antiparticles (-) are listed for proton and neutron targets. In the Mueller-Regge picture the difference in the π^+ and π^- rates for proton targets together with the approximate equality for neutron targets can be explained by ρ and ω exchanges which interfere constructively for protons and cancel for neutrons.

Brodsky and Gunion (37) explain the π^+/π^- ratio as a valence quark effect. The basic scattering process is $\gamma q \rightarrow q$ in contrast to the usual assumption $\gamma, q \rightarrow q$ for virtual photons. In this context it might be interesting to note, that also the π^{\pm}/π^0 ratio is a function of p_{\perp} . This can be seen in fig. 28, where the data of ref.27 are plotted together with the results of a DESY (36) group for the reaction $\gamma p \rightarrow \pi^0 X$ in the beam fragmentation region. In electroproduction the π^0 rate is given by the average of the π^+ and π^- rate as requested by the quark parton model (43). It would be certainly interesting to have a better understanding of the ratio π^0/π charged in photoproduction.

TABLE 1 COMPTON SCATTERING

	$ T_0 ^2$	$\frac{\text{Re}(T_0 T_1^*)}{ T_0 + T_1 ^2}$
DESY 5 GeV	$.13 \pm .09$	$0. \pm .03$
DESY 6 GeV (ref. 6)	$-.12 \pm .15$	$.10 \pm .04$
SLAC (8 and 16 GeV) (ref. 17)	$.03 \pm .10$	$-.043 \pm .012$
average	$0.08 \pm .05$	0.02 ± 0.01

TABLE 2 COUPLING CONSTANTS

V	$f_V^2 / 4\pi$
ρ	$2.55 \pm .28$
ω	18.4 ± 1.8
ϕ	12.15 ± 1.1
ψ	11.45 ± 1.43
(ρ')	17.5 ± 5

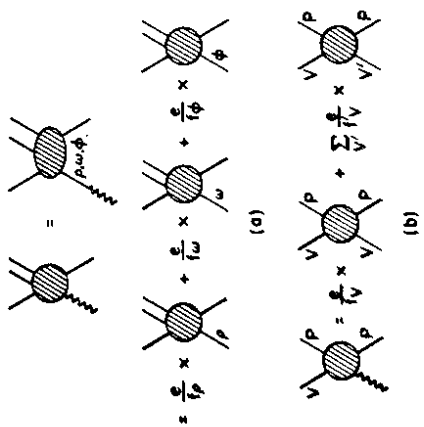


Fig.1: Vector Meson Dominance diagrams

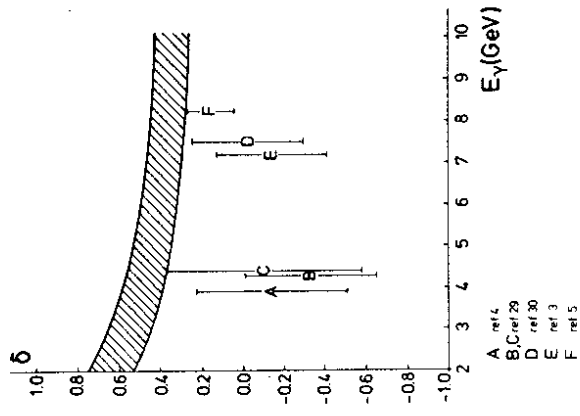


Fig.2: Measurement of $\delta = \text{Im } A_1 / \text{Im } A_0$ for ω production in forward direction. Fig. taken from ref. 4.

TABLE 3 4 RES. FIT TO $\gamma p \rightarrow e^+ e^- p$ (ref. 39)

M_V	Γ_V	$\frac{1}{f_V^2 / 4\pi}$	$\frac{d\sigma}{dt} _{t=0}$	ϕ
MeV	MeV	$\mu\text{b}/\text{GeV}^2$		degrees
1253 ± 16	120 ± 38	$.04 \pm .025$		6.8
1401 ± 9	134 ± 18	$0.25 \pm .05$		11.0 ± 9.0
1549 ± 26	230 ± 21	$.22 \pm .06$		1.2 ± 6.0
1766 ± 8	139 ± 30	$.15 \pm .04$		29.0 ± 5.0

TABLE 4 REGGE EXCHANGE AMPLITUDES

	$p\pi^+$	$p\pi^-$	$n\pi^+$	$n\pi^-$
P, f	+	+	+	+
ω	+	-	+	-
ρ	+	-	-	+
A_2	+	+	-	-

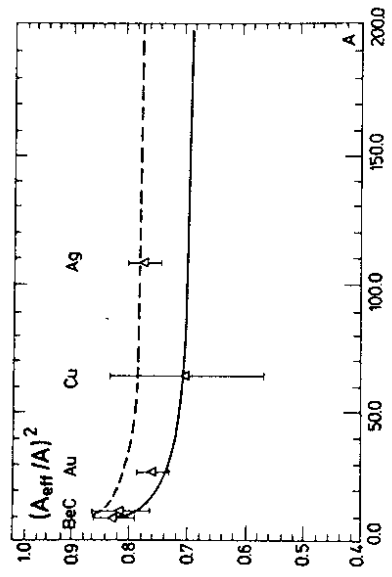


Fig.3a: Compton scattering on complex nuclei. Fig. taken from ref.9.

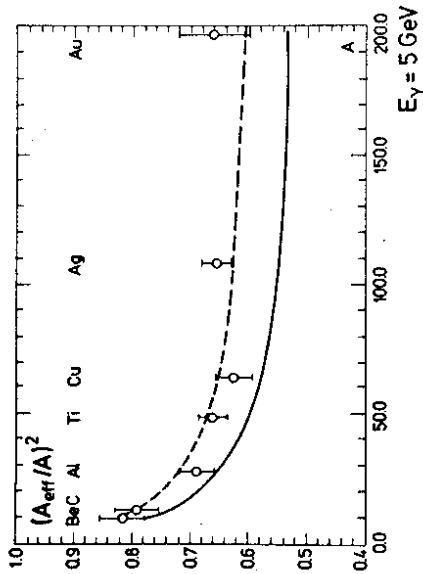


Fig. 3b: Compton scattering on complex nuclei, fig. taken from ref. 9.

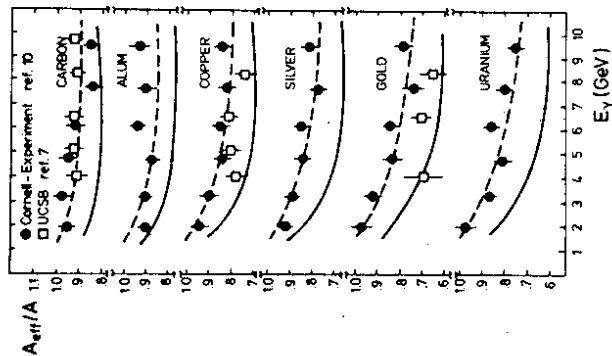


Fig. 4: Shadowing factor A_{eff}/A against E_γ . Fig. taken from ref. 11.

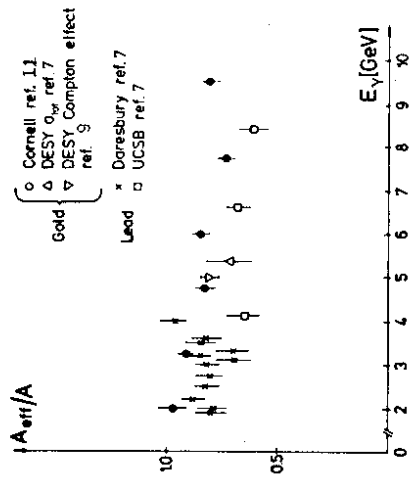


Fig. 5: Shadowing factor A_{eff}/A against E_γ for heavy elements.

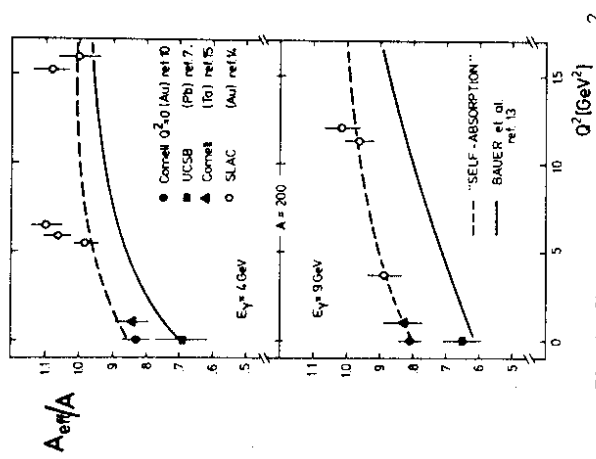


Fig. 6: Shadowing factor versus Q^2 . Fig. taken from ref. 11.

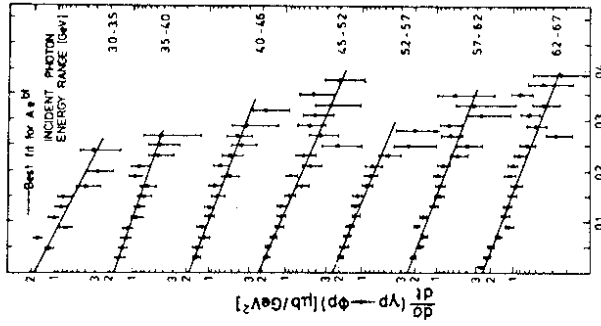


Fig. 7: $d\sigma/dt$ for ϕ production at various energies. Fig. taken from ref. 21.

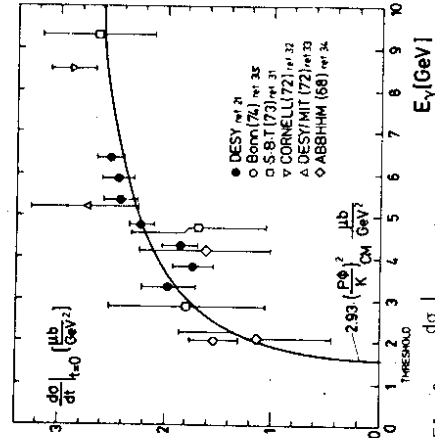


Fig. 8: $\left. \frac{d\sigma}{dt} \right|_{t=0}$ for ϕ production versus E_γ , fig. taken from ref. 21.

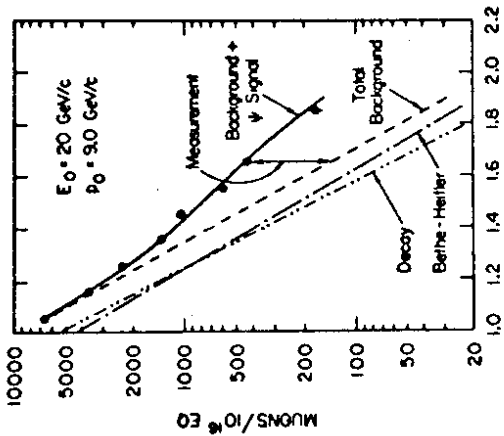


Fig. 9: Muon yield versus transverse momentum for ψ production on beryllium, fig. taken from ref.19

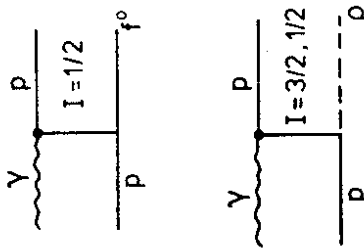


Fig. 10: Exchange diagrams for backward production of f_0 and ρ_0

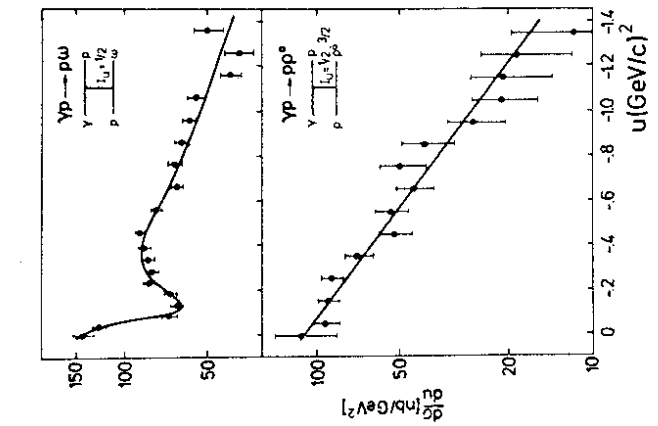
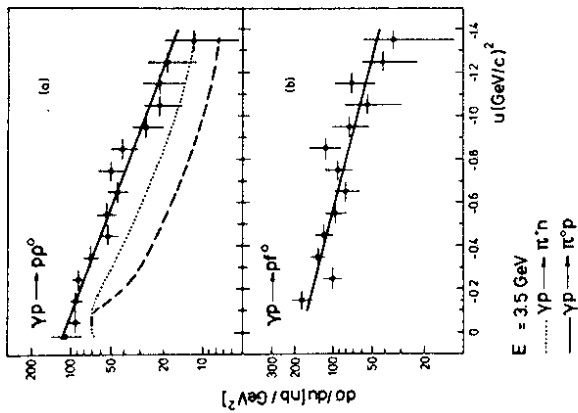


Fig. 12: $\frac{d\sigma}{du}$ for backward ρ_0 and f_0 photoproduction (ref.20)

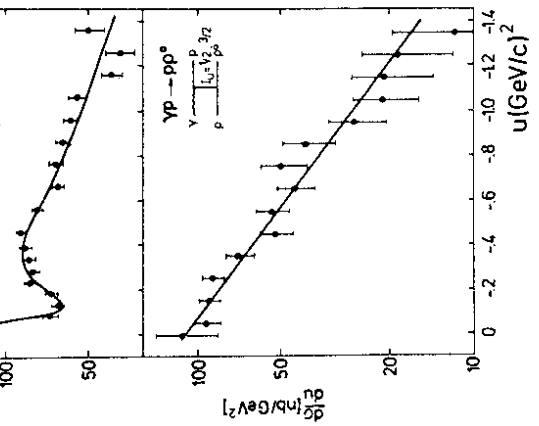


Fig. 13: $\frac{d\sigma}{du}$ for backward ω production (ref.22)

Fig. 14: Inclusive structure function $F(x)$ for p photoproduction. Fig. taken from ref.25.

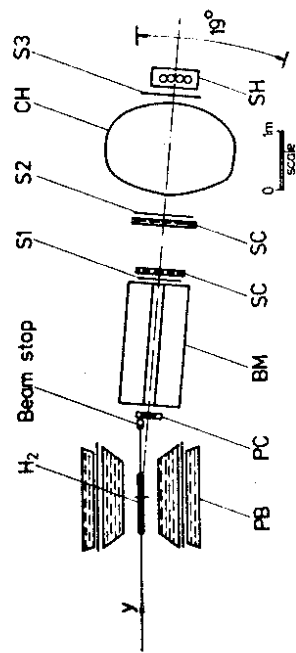


Fig. 11: Layout of the spectrometer used in the backward f_0 and ρ experiment.

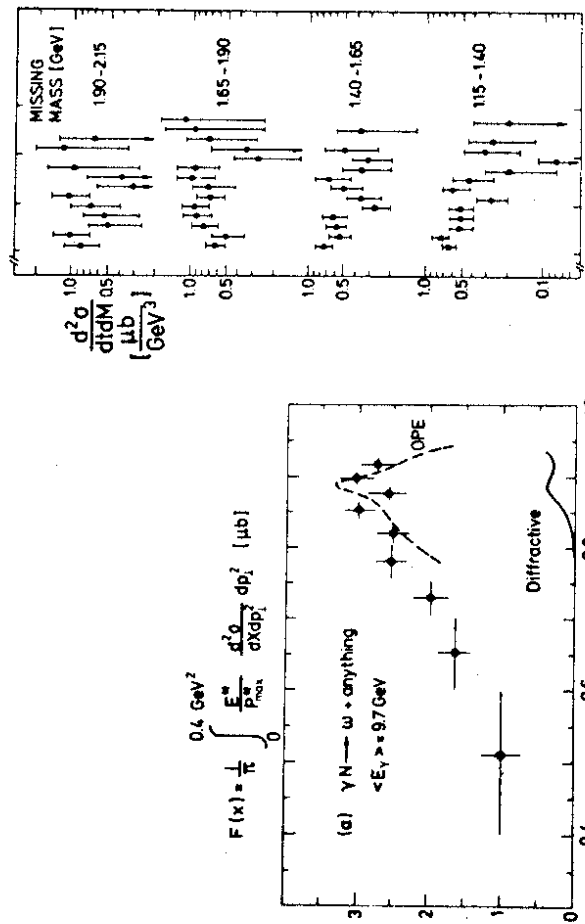


Fig.15: Inclusive structure function for ω photoproduction (ref. 26)

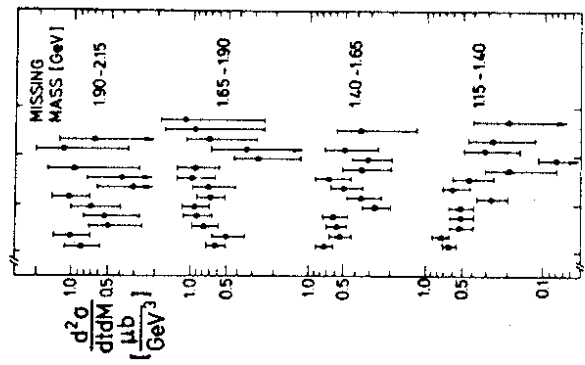


Fig.16: $d\sigma/dt dM^2$ for inelastic ϕ meson photoproduction (ref. 21)

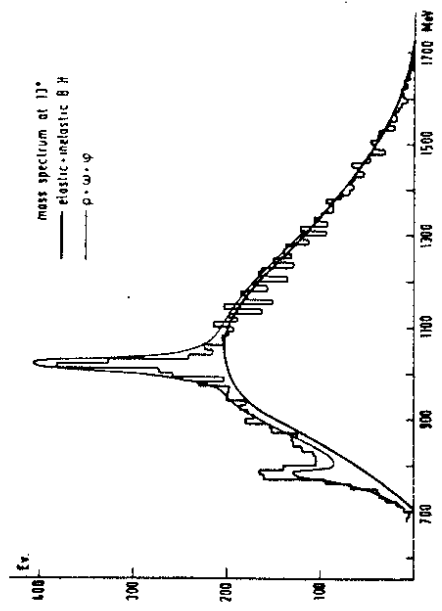


Fig.18: Invariant mass spectrum of e^+e^- pairs.

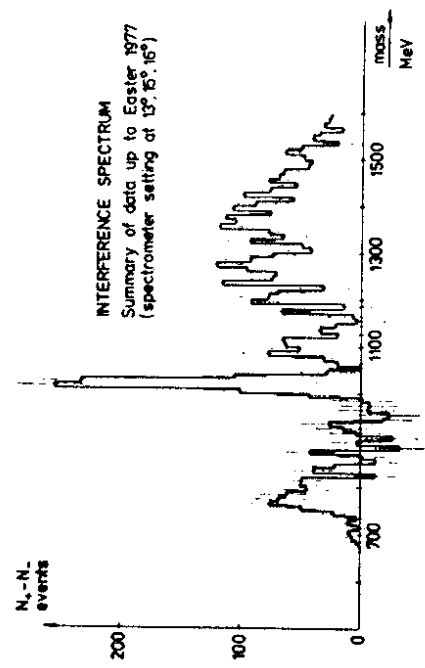


Fig.20: Interference spectrum (Bethe-Heitler and Compton amplitude) obtained in the DESY-Frascati experiment (ref. 39).

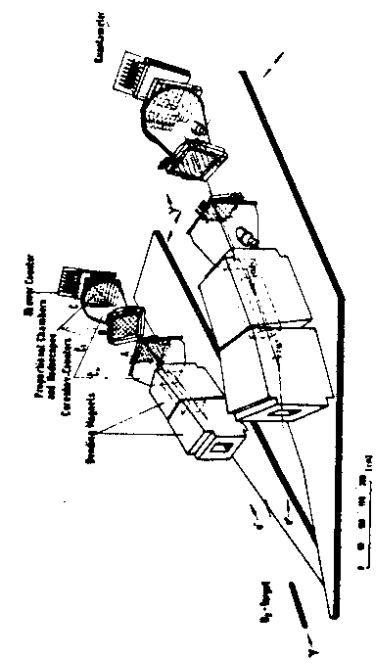


Fig.17: Apparatus used in the DESY-Frascati experiment (ref. 39)

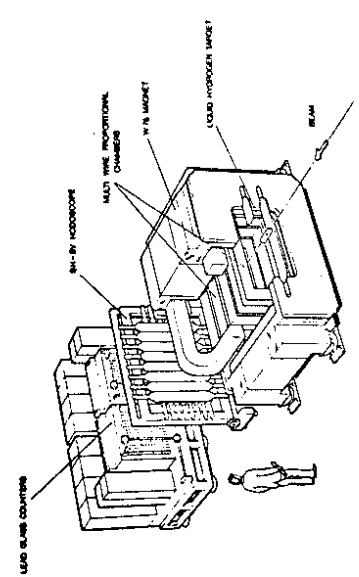


Fig.21: Multiparticle spectrometer at Daresbury.

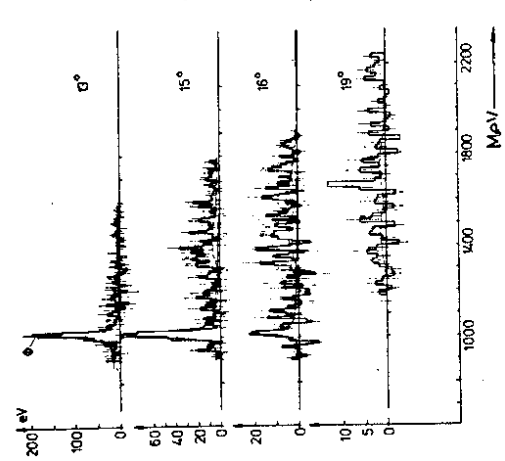


Fig.19: Invariant mass spectrum of the e^+e^- pairs at various opening angles of the spectrometers (ref. 39)

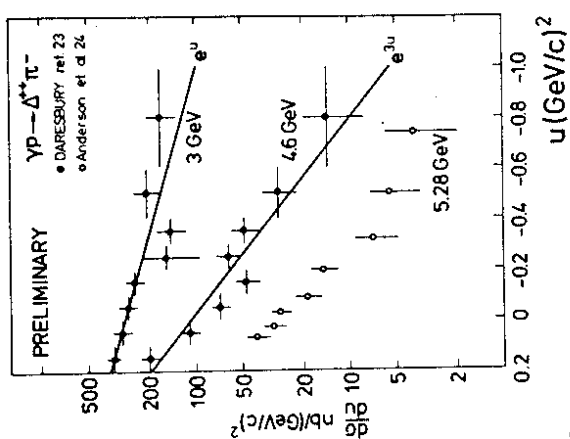


Fig.22: Cross section for $\gamma p \rightarrow \pi^+ \pi^+$ in backward direction. Fig. taken from ref. 23.

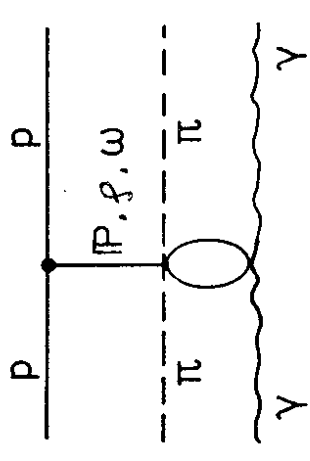


Fig.23: Muller-Regge diagram for inclusive pion photoproduction.

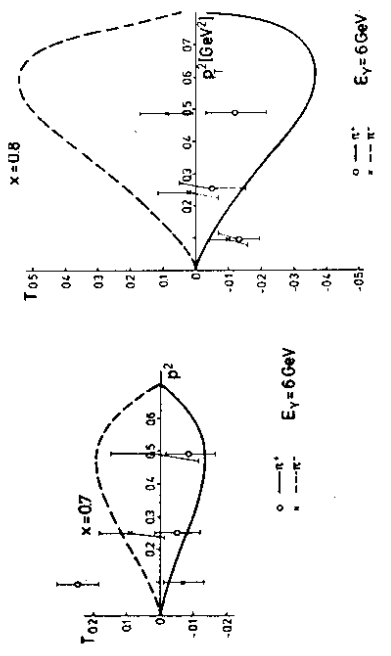


Fig.24: Target asymmetry in inclusive pion photoproduction (ref. 42)

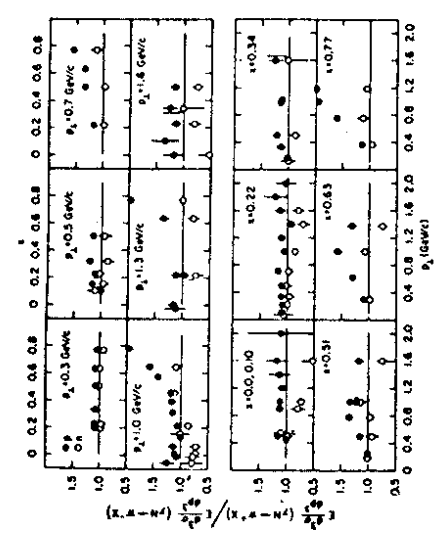


Fig.25: π^+/π^- ratio in photoproduction (ref.28)

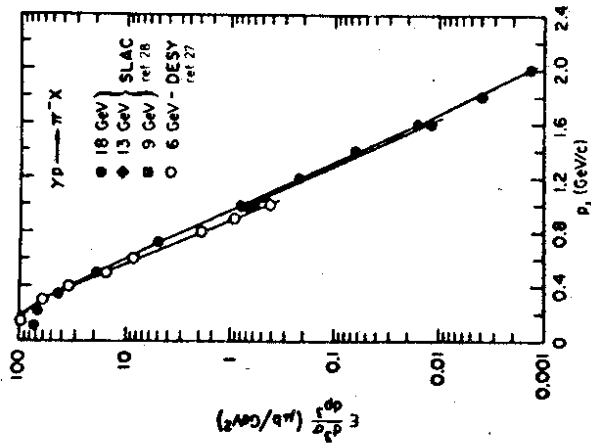


Fig.26: Invariant cross section for $yp \rightarrow \pi^+ X$ Fig. taken from ref. 28

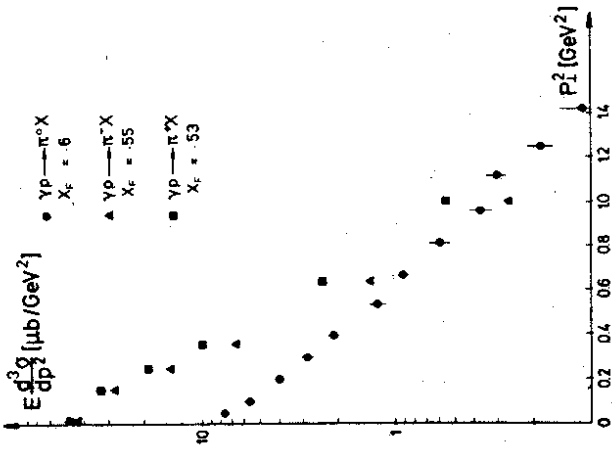


Fig.27: Invariant cross section for $yp \rightarrow \pi^+ X, yp \rightarrow \pi^+ X$.

12. R. Talman PR D15 (1977) 1260
13. T. Bauer et al., Rev. Mod. Phys. (to be published)
14. S. Stein et al. PR D12 (1975) 1884, W.R.Ditzler PL 37B (1975) 201
15. J. Eickmeyer et al. PRL 36 (1976) 289
16. See M.M. Nagles et al. NP B109 (1976) 1 and ref. quoted there.
17. A.M. Boyarski et al. PRL 26 (1971) 1600, 30 (1973) 1098
18. T. Bauer and D.R. Yennie PL 60B (1976) 165, 169
19. R.L. Anderson et al. PRL 38 (1977) 263
20. R.W. Clifft et al., PL 64B (1976) 213
21. H.J. Behrend et al., paper submitted to NP B, part of the results published in PL 56B (1975) 408
22. R.W. Clifft et al. Paper prepared for publication, private communication by R. Marshall
23. D.P. Barber et al. paper prepared for publication, private communication by R. Marshall
24. R. I. Anderson et al. PRL 23 (1969) 721
25. E. Kogan et al. SLAC PUB 1857 (1976)
26. C.A. Neilson et al., paper submitted to PR
27. H. Burfeindt et al., NP B74 (1974) 189
28. A.M. Boyarski et al. PRD 14 (1976) 1733
29. Y. Eisenberg et al. NP B42 (1972) 349
30. G. Alexander et al. PL 57B (1975) 487
31. J. Ballam et al. PR 7D (1973) 3150
32. C. Berger et al. PL 39B (1972) 659
33. H. Alvensleben et al. PRL 28 (1972) 66
34. ABBHM, PR 175 (1968) 1669
35. H.J. Besch et al. NP B70 (1974) 237
36. C. Berger et al. PL 47B (1973) 377
37. S. Brodsky and J.F. Gunlon e.g. In SLAC PUB 1820 (1976)
38. G. Wolf NP B26 (1971) 317
39. S. Bartolucci et al. DESY 76/43 NC 39A (1977) 374 and paper submitted to the conference
40. A.H. Mueller, PRD 2 (1970) 2963
41. K. Ahmed et al. DESY 75/39 (1973)
42. H. Genzel et al., paper prepared for publication, H. Genzel private communication
43. C. Berger et al., paper submitted to PL

REFERENCES

1. For a review see e.g. G.Wolf In Proceedings of the 1971 Internat. Symp. on Electron and Photon Interactions, Cornell University, Ithaca, N.Y.
2. H. Harari In Proceedings of the 4th Internat. Symp. on Electron and Photon Interactions at High Energies, Liverpool, 1969
3. H.J. Behrend et al. PRL 26 (1971) 151
4. J.V. Morris et al. NP B119, (1977), 420
5. J. Abramson et al. PRL 36 (1976) 1428
6. L. Crlegee et al. NP B121 (1977) 31
7. For a review see e.g. A. Silverman In Proceedings of the 1975 Symp. Lepton and Photon Interactions at High Energies, Stanford, 1975
8. For a very good discussion see K. Gottfried In Proceedings of the 1971 Internat. Symp. on Electron and Photon Interactions, Cornell University, Ithaca, N.Y.
9. L. Crlegee et al. NP B121 (1977) 38
10. K. Gottfried et D.R. Yennie PR 182 (1969) 1595 and ref. 15 quoted in ref.9
11. S. Michalowski et al., CLNS Preprint 361, Cornell University